

Field-Emission Properties in the ERL-Electron Source

Vaibhav Kukreja

Department of Physics, Cornell University, Ithaca, New York, 14853

(Dated: August 10, 2005)

One concern around the development of the electron gun for the next generation linear accelerator, namely ERL (Energy Recovery Linac), is finding a suitable material and surface preparation technique to construct the cathode of the electron gun. With the hope to run the electron gun at an electrostatic field of 15 MV/m (750 kV over a 5 cm gap), electron field emission poses many risks to the function and the structure of the gun. We have tested five electrodes with different composition and surface treatment. In this paper, we will discuss their emission behavior, and briefly introduce and apply the Fowler-Nordheim field emission theory to determine the enhancement factors and emission areas for the examined samples. The Bare Titanium sample has shown dramatic results with no field emission up 21 MV/m. This might be a strong candidate for the material composition of the cathode.

I. INTRODUCTION

Electron field emission imposes a great restriction on the operating voltage of electron guns. In recent years, there has been an appeal to construct DC electron guns based on photoemission cathodes and use cathode fields that are significantly higher than what today's guns operate at (well below 10 MV/m). The motivation for having electron sources with such high field strengths is primarily based on the hope that they can yield high brightness and high average current beams [3]. These features are very important for the energy recovered superconducting linear accelerators such as the ERL and for future applications in light sources, electron cooling and electron-ion colliders.¹ With all of these positive outlooks from using very high cathode fields, the risk of heavy electron field emission is a serious concern.

Field emission from the cathode electrode puts a serious constraint on the field strength of the electrode and respectively on the operating voltage of the DC electron gun. The emission electrons pose many dangers to the gun's function and its structure. For instance, the field-emitted electrons can cause charging, which can lead to the breakdown of the ceramic insulator and seriously damage the support of the cathode. Also the emission electrons can cause melting of the materials they clash with and this can lead to arcing or structural breakdowns inside the gun. Moreover, electrons from field emission induce certain gases when they strike materials. These gases can chemically damage the high quantum efficiency photocathodes and produce residual gas, causing ion back bombardment and harming the photocathode [3].

Our knowledge of electron field emission, especially from large area electrodes under the influence of high DC voltage, is remarkably small. It is extremely difficult to select electrode materials and surface treatments that would insure a stable performance of the DC gun with high voltage and high anode-cathode field strength [3]. To get around this

¹ See Sinclair et al. for a detailed discussion on photoemission cathode and high cathode field. [3]

difficulty, in 2001, C. Sinclair and others at the Thomas Jefferson National Accelerator Facility (TJNAF) reported that they have developed a unique apparatus to test the field emission and processing (or conditioning) behavior of large surface electrodes [3]. Under the guidance of C. Sinclair, a similar experimental chamber was built at the Laboratory for Elementary Particle Physics (LEPP) at Cornell University for our tests. Along with the physical design of the test chamber, many other attributes (such as voltage and electrode characteristics) of the experiment done at TJNAF were repeated for our tests (discussed in the Experimentation section).

II. FIELD EMISSION: THEORY AND HISTORY

Electron Field Emission or Fowler-Nordheim quantum mechanical tunneling is the process of releasing electrons from metal surface via barrier penetration in the presence of a high electric field. Unlike the escaping over a potential barrier as with photoemission and thermionic processes, field emission is purely a quantum mechanical phenomenon. The theory of electron field emission was formally published in 1928 by Fowler and Nordheim. Initially there was not much progress made with this theory outside the realm of pure science. However, this certainly changed in 1937 when Erwin Muller first used this phenomenon on the experimental front and devised a new way to do microscopy [1]. Muller was successfully able to use the extracted electrons from a field-emitting metal tip to create an image of the tip, revealing its surface structure.

The Fowler-Nordheim model for field emission describes the electron current density J emitting from a surface into vacuum as a function of the applied field E . The model parameters that govern the emission are the material (effective work function, ϕ), the area available for emission A_e and a geometric enhancement factor β . B_1 and B_2 are known fundamental constants, I is the prebreakdown current, and gap distance d . The enhancement factor describes how electric fields can be enhanced by protrusions from the emitting surface [2].²

Emission Current Density with local surface field E is given by

$$J = (B_1 E^2 / \phi) \exp(-B_2 \phi^{3/2} / E) \quad (1)$$

Under the assumption that there is one major site of field emission and its emitting area denoted by A_e and with $E = \beta(V/d)$ accounting for enhancement where V is the applied voltage, the total prebreakdown current I as $I = JA_e$ in logarithmic form is given by

$$\log(I/V^2) = (dB_2 \phi^{3/2} / \beta)(I/V) + \log(A_e B_1 \beta^2 / d\phi) \quad (2)$$

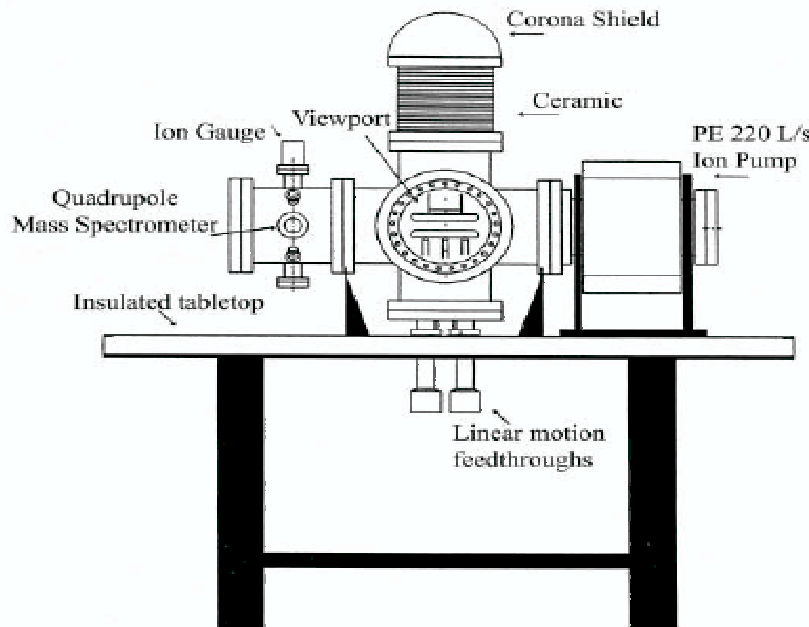
The Complete Fowler-Nordheim Result:

$$\log(I/V^2) = \log \frac{1.54 \times 10^{-6} A_e \beta^2 10^{4.52\phi^{-0.5}}}{\phi d^2} - \frac{2.84 \times 10^9 d \phi^{1.5}}{\beta} \frac{1}{V} \quad (3)$$

² See chapter 4 of Latham for the full derivation of the Fowler-Nordheim result. [2]

III. EXPERIMENTATION

As previously mentioned, our experimental chamber is a duplicate of the test chamber described in [3]. For the reader's reference, a schematic view of the apparatus is given below in Fig 1. For brevity, certain details on the test chamber are omitted hereafter. The reader is welcome to check the reference above for specific details on the design of the test chamber.



A Schematic view of the electrode test chamber.

Essentially, the experimental chamber is built around a stainless steel six-way vacuum cross. The entire apparatus stands on a thermally insulated table for convenient bakeout of the chamber. The ceramic insulator sits on top of the cathode and it is electrostatically protected. The apparatus can safely operate up to 125 kV with appropriate shielding around it. An ion pump along with a turbo pump (not shown in Figure 1) is used to pump away the residual gases and other contaminants from the chamber. To measure the pressure level of residual gases inside the chamber, a RGA (Residual Gas Analyzer) is used. Both electrodes, the cathode and the anode, are geometrically similar with the plane-parallel gap between them. The cathode is arranged on a circular tube (three inches wide) and the anode held in place by a weight. The anode is connected to three screws, which can be used to set and align the gap between the cathode and the anode. In addition to the apparatus above, two optical instruments are used to get a precise measurement of the gap between the electrodes. All bakeouts are performed at 250 C over a 24-hour period.

All the tested electrodes have the same geometry. The anode and the cathode are both disc-shaped (area of 100 cm^2) with a quasi-Rogowski profile. This profile helps to reduce the edge effects that result from the increase in the electric field at regions with sharply curved edges on the electrode [2]. For all the tested samples, the anode was Ti4V6A1. This is a common Titanium alloy for structural applications with composition of 90% Ti, 6% Aluminum,

and 4% Vanadium. The surface of the anode was prepared using a chemo-mechanical polishing technique. The anode electrode was first hand polished with diamond paste to a 6-9 μm surface finish. Then, the sample was polished with a solution of hydrogen peroxide and 0.05 μm colloidal Silica (SiO_2). As for the cathode electrodes, they form an eclectic group with their composition and surface treatment. The five tested cathode electrodes are 316 Stainless Steel, Beryllium Copper, 304 Stainless Steel, Ti4V6A1 (differently treated from the anode), and Bare Titanium (with same makeup as the Ti4V6A1 alloy), and hereafter denoted as 316LN, CuBe, SS#5, Ti#4, and Ti#3 respectively. All of the electrodes were polished at Wilson Laboratory, and the surface of SS#5 and Ti#4 electrode was coated at Epion (see [5] on the Epion process).

The electrodes were tested in a clean, dust free environment to minimize the contamination of the electrode and consequently reducing the possibility of significant field emission. Furthermore, dry nitrogen was used to blow off the surface of the electrode and remove specks and other contaminants from the handling and air exposure. Nevertheless, a complete removal of all such air particles is nearly an impossible task. Before a cathode electrode is changed, the test chamber is vented with N_2 and pumped with the turbo pump. After the electrode is replaced, the ion pump is started and the bake out follows. At the conclusion of the bake out, the test chamber is checked for leaks and a suitable vacuum level (usually 10^{-10} torr) is achieved. There are two phases involved in testing the emission behavior of the electrodes. During the day, current conditioning is applied to the sample electrode. The values for prebreakdown current and power supply voltage are recorded. After the day run, the electrode is quickly retested with the applied voltage increased in increments of 4 kV or 5 kV up to the maximum voltage reached in the days run. Once again, the quantities of prebreakdown current and power supply voltage are measured. The prebreakdown currents are measured with a Keithley picoammeter. Several samples were tested multiple times. Each time, the current conditioning and the after day run-up were applied to the electrode.

IV. PREBREAKDOWN CURRENT AND CURRENT CONDITIONING

The phenomenon of prebreakdown current is extremely complex and as a result, only vaguely understood. Essentially, it is the response of the current as the voltage is put on the electrode. There are two types of prebreakdown currents: unstable and stable. The unstable prebreakdown currents are by nature very noisy. They are composed of sharp current pulses called microdischarges pulses. At present, there are several explanations on the origin of unstable prebreakdown currents. One principal reasoning for the occurrence of this phenomenon is explosive electron field emission. Other causes for prebreakdown behavior are the regenerative ionization process and the ion-exchange mechanism [2]. The first of these physical processes involves desorption of residual gases present in the chamber after the bakeout. The latter process involves the generation of ions from the contaminant films on the electrode surface. Meanwhile, stable prebreakdown currents emerge from a cold emission process at one or two points on the electrode. However to get the electrode at this stage, the current conditioning has to be applied. In general, the purpose of electrode conditioning is to remove the sites of prebreakdown currents (so-called primary microparticle events) in order to achieve a stable voltage gap. There are common four types: current conditioning, glow-discharge conditioning, gas conditioning, and spark conditioning. Since the current conditioning is most germane to our discussion and tests, we will not discuss

the others.³ Current conditioning is a simple and fairly efficient method to process the electrode. In this routine, the voltage is applied in small steps to the cathode electrode. While at each voltage amount, the experimenter waits until the prebreakdown current settles or stabilizes before proceeding further. A common characteristic of this conditioning is the permanent drop in the average value of the prebreakdown current. There are three physical processes behind the stabilizing effects of current conditioning [2]. The first one concerns with the thermal blunting of heavy electron emission sites (called microprotusions) and sometimes a complete removal of these sites by the electro-magnetic forces. Secondly, the removal of poorly attached microparticles on the electrode surface also helps to steady the prebreakdown current. Lastly, the desorption of remnant gases is also another important factor behind the current stabilization.

V. RESULTS

We are reporting measurements on five sample electrodes. All the figures below are showing the emission behavior of the electrodes after the current conditioning was applied to them. The first electrode, namely 316LN, is composed of stainless steel. More precisely, it is primarily iron, with 18% chrome and 12% Nickel (the additional nickel makes it even less prone to corrosion). The surface was hand polished with diamond paste to a 1 μm finish. The second sample electrode, namely CuBe, is copper alloy and its makeup is 99% Cu and less than 1% Be. The Beryllium is used to harden the soft copper. The third sample is another stainless steel electrode, namely SS#5, with a little different composition from the 316LN electrode. It is mainly iron, with 18% Chrome and 8% Nickel. Like the 316LN sample, SS#5 was also hand polished with diamond paste to a 1 μm . The surface of this electrode was further treated with a coating done by the Epion procedure, which comprises of bombarding the electrode sample with ion clusters composed of 15000 or more atoms [5]. The fourth tested electrode, namely Ti#4, has the same structural makeup as the anode (discussed under Experimentation). The surface treatment for this electrode consisted of titanium nitride coating done with the Epion process. The fifth and the last tested sample is Bare Titanium, denoted as Ti#3, also with the same composition as the anode. The surfaces of both the Ti#4 sample and the Ti#3 sample were done using the chemo-mechanical polishing technique (described in the Experimentation section).

The field emission behavior of the 316LN sample was quite good, see figure 2. After two days of current conditioning, the electrode had barely any field emission up to a gap field of 16 MV/m. We gained almost 2 MV/m from day 1 after the conditioning and processing. In addition, the sample was tested at a larger gap and had minor field emission activity up to 16 MV/m again. The next sample, CuBe, was not at the level of 316LN. After the conditioning, the emission behavior worsened as the sample was field emitting at 10 MV/m, see figure 3. Meanwhile during the conditioning, the sample reported no field emission up to 13 MV/m. The emission behavior for SS#5, the stainless steel electrode prepared by Epion, was in between of 316LN and CuBe. On day 2, the sample indicated no field emission up to 14.5 MV/m (see figure 4), which was a little better from day 1 with emission occurring at 14 MV/m. However, further testing on day 3 showed considerable conditioning progress, but on day 4, the sample had field emission at 10.5 MV/m. The titanium nitride coated

³ See Chapter 2 of Latham for a comprehensive discussion on conditionings. [2]

electrode, Ti#4, had emission field performance similar to that of the SS#5 electrode. This sample showed very little sign of field emission up to 14 MV/m (see Figure 5) and it was by far the most conditioned and processed sample. To check whether the earlier results of 316LN will stand the test of time, the 316LN sample was retested ⁴ and the emission behavior is displayed in figure 6. Although it began comparable to the earlier performance, significant amount of microdischarges appeared around 13 MV/m during the conditioning and thereafter current became very noisy and unstable. After the conditioning, the sample was field emitting at 14 MV/m. The last tested sample, bare titanium (Ti#3), was the most exceptional piece. The hand-polished electrode produced no field emission up to a noteworthy gap field of 21 MV/m (see Figure 7). However, at a field of about 23 MV/m, the current suddenly jumped up almost four orders of magnitude. Hence, the conditioning for this electrode was not completed.

Figure 8 show an example of Fowler-Nordheim plot, where the measured values of pre-breakdown (I) and voltage (V) were used to make a plot of $\log(I/V^2)$ vs. (I/V) . From these plots, the slope and the intercept were calculated to respectively determine from the Fowler-Nordheim result [Equation (3)] the enhancement factor (β) and the emission area (A_e) for each cathode electrode (while and after the current conditioning). Table I and II on pg. 9 summarize these results. (Consult the Discussion and Comparisons section for further details.) It should be noted that the enhancement factor and emission area values for Ti#3 or bare titanium are not present in these tables since its conditioning was not finished.

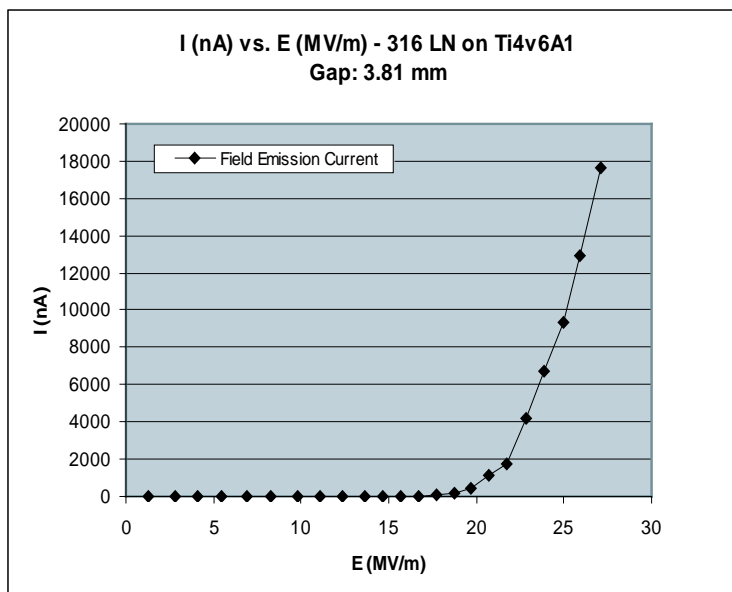


Figure 2: Emission behavior from the 316LN stainless steel

⁴ Denoted as 316LN-R in Table I and Table II

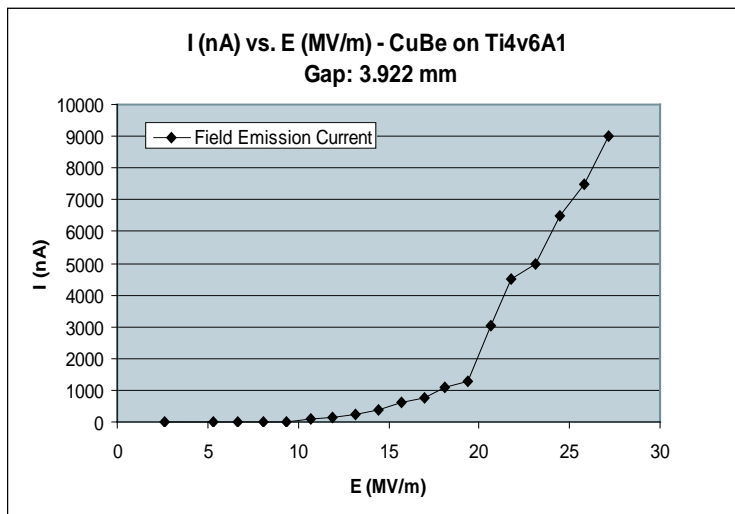


Figure 3: Emission behavior from the CuBe copper alloy

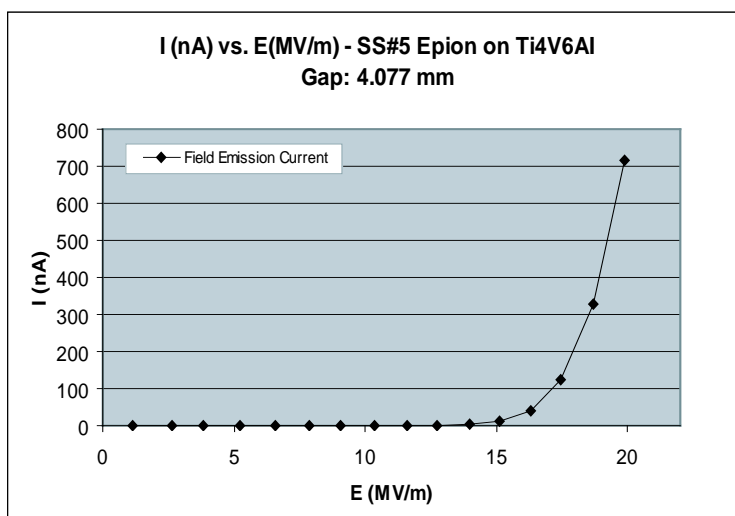


Figure 4: Emission behavior from the Epion prepared SS#5 stainless steel

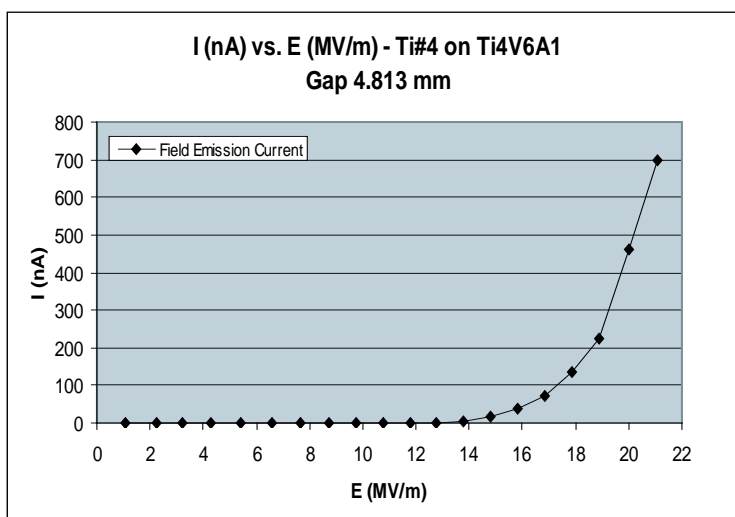


Figure 5: Emission behavior from the Ti#4 titanium alloy

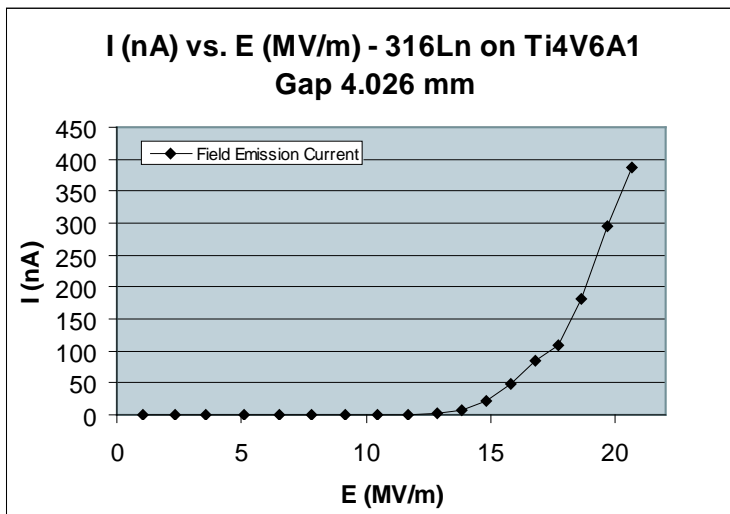


Figure 6: Emission behavior from re-run of 316LN stainless steel

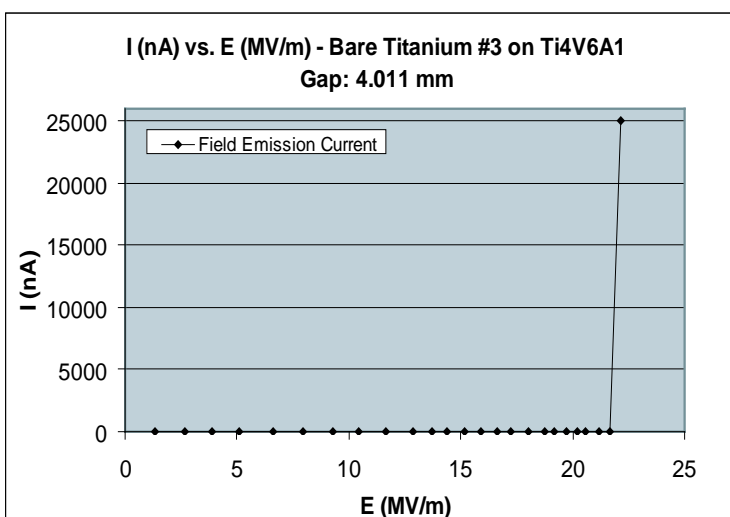


Figure 7: Emission behavior from Ti#3 bare titanium

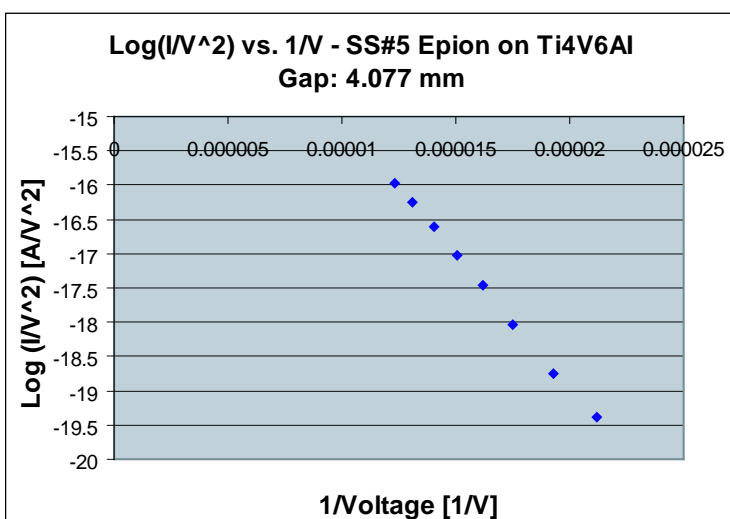


Figure 8: A Sample Fowler-Nordheim Plot

TABLE I: Enhancement Factors (β) and Emission Areas (A_e) while Current Conditioning

Electrode	Day	Gap (m)	$\phi(eV)$	Slope (A/V)	Intercept (A/V ²)	β	$A_e(m^2)$
316LN	1	0.00381	4.5	-33844	-11.058	305	2.9496E-17
316LN	2	0.00381	4.5	-35917	-11.165	288	2.5940E-17
316LN	3	0.005042	4.5	-38634	-12.565	354	1.1954E-18
316LN-R	1	0.004026	4.5	-20129	-13.939	542	1.3710E-20
CuBe	1	0.003922	4.65	-17563	-13.597	636	2.3303E-20
SS#5	1	0.004077	5	-30234	-12.027	428	2.6347E-18
SS#5	2	0.004077	5	-40996	-10.878	316	6.8214E-17
SS#5	3	0.004077	5	-32002	-12.233	405	1.8374E-18
SS#5	4	0.004077	5	-22916	-12.396	565	6.4611E-19
Ti#4	1	0.004813	4.33	-10591	-13.951	1163	3.6272E-21
Ti#4	2	0.004813	4.33	-12735	-15.012	967	4.5529E-22

TABLE II: Enhancement Factors (β) and Emission Areas (A_e) after Current Conditioning ^a

Electrode	Day	Gap (m)	$\phi(eV)$	Slope (A/V)	Intercept (A/V ²)	β	$A_e(m^2)$
316LN	1	0.00381	4.5	-46109	-9.6497	224	1.4013E-15
316LN	2	0.00381	4.5	-50851	-9.5329	203	2.2304E-15
316LN	3	0.005042	4.5	-76024	-8.5754	180	4.5204E-14
316Ln-R	1	0.004026	4.5	-27158	-12.865	402	2.9623E-19
CuBe*	1	0.003922	4.65	-17563	-13.597	636	2.3303E-20
CuBe	1	0.003922	4.65	-13164	-13.716	848	9.9507E-21
SS#5	1	0.004077	5	-41498	-10.771	312	8.9455E-17
SS#5	2	0.004077	5	-39481	-11.085	328	3.9320E-17
Ti#4	2	0.004813	4.33	-33854	-12.776	364	5.5409E-19

^aFor a comparison, we have put Cube* in Table II to indicate the values from during the current conditioning.

VI. DISCUSSION AND COMPARISONS

One thing that Tables I and II assure us of is the success of current conditioning. The enhancement factor is a measure of protrusion geometry. As discussed earlier, current conditioning can certainly weaken and sometimes completely remove these emission-causing agents. For all samples, except the CuBe, the sizes of enhancement factors (β) were reduced after the electrode conditioning. In some cases, these drops were quite significant. For instance, the Ti#4 electrode experienced a fall of almost 900 in its enhancement factor value. The 316LN sample achieved the lowest enhancement factor of 180. Common values for enhancement factor and emitting area are $100 < \beta < 1000$ and $10^{-16} < A_e < 10^{-12} m^2$ respectively [2]. Although our values of enhancement factors are well within their typical range (definitely after the current conditioning), the emitting areas are coming to be much smaller and quite away from the range mentioned above. This in fact is one of the classical shortcomings of the Fowler-Nordheim model. The source of this drawback is rooted in the assumption that there is a single point of field emission on the electrode surface.

Earlier tests done on the stainless steel electrode and Ti4V6A1 (both *only* hand polished with diamond paste up to a 1 μm surface finish) by C. Sinclair and others at TJNAF have reported no major field emission up to 11 MV/m and 16 MV/m respectively [3]. The first sample is most comparable to our 316LN Stainless Steel electrode (also hand polished in a similar way) which has withstood up to 16 MV/m of gap field with no significant emission. The Ti4V6A1 electrode or Ti#4 (for our tests the sample was first treated with a chemo-mechanical polishing technique and then coated with titanium nitride by Epion) only held out field emission until 14 MV/m. On the other hand, the Ti#3 or bare titanium sample (just with chemo-mechanical polishing) has definitely surpassed the performance of 16 MV/m from the same alloy tested at TJNAF. Furthermore, C. Sinclair also tested ion implanted stainless steel electrodes, which had no field emission up to 20 MV/m and showed signs of very little emission at a gap field of 30 MV/m [3]. Certainly, the bare titanium is the only candidate from our list of tested electrodes that can serve as any match for these electrodes. However, with heavy field emission occurring at only 23 MV/m indicates that the bare titanium sample is also well short of the emission performance from the ion implanted electrodes. Nevertheless, we certain that our chemo-mechanical polishing has dramatically improved the performance of the titanium samples.

VII. CONCLUSIONS

From these tests we have made progress towards a better understanding of surface preparation and composition of electrodes. Firstly, the 316LN sample shows that we have certainly learned how to polish metal at Wilson Lab. Also from these tests, we know that CuBe, a copper alloy, poses a high risk of field emission. We cannot use copper in electrodes. This to some extent is bad news (since copper is great for heat conduction and for removing the excess heat generated on the cathode from laser illuminating the photocathode), but this information has saved a *lot* of time and money. Last of all, the Epion process seems promising. We have attained quite decent results from poorly polished samples. Our results are showing that we might be close to finding the appropriate composition and surface preparation for the cathode of the electron gun. The exceptional performance of bare titanium might be enough to satisfy the requirement of 15 MV/m, however the abrupt and significant jump observed in the current is something we need look at more closely. Nevertheless, we surely need to test more samples and gain insight into how the electrodes and their gap performance change overtime. This is crucial for samples such as the 316LN stainless with the loss of 2 MV/m after the re-test. On the mathematical front, we have to understand the nature of enhancement factors and try to get agreeable values for the emitting areas. For the last goal, we may be need to look at more advanced theories of field emission such as the multielectron theory of field electron emission [4].

VIII. ACKNOWLEDGMENTS

I am greatly indebted to Dr. Charles Sinclair of the Laboratory for Elementary-Particle Physics at Cornell University, whose immense help and guidance made these important tests happen. I would also like to thank Dr. Georg Hoffstaetter and Dr. Richard Galik for giving me the privilege to take part in the REU program. Last, but certainly not least, I am very grateful to Karl Smolenski and Dr. Ivan Bazarov for helping me to gather and understand

the experimental results.

This work was supported by the National Science Foundation REU grant PHY-0243687 and research co-operative agreement PHY-9809799.

-
- [1] French and Taylor, An Introduction to Quantum Physics Norton, W. W. Company, Inc., New York, 1990.
 - [2] R. V. Latham, High Voltage Vacuum Insulation Academic Press, London, 1995.
 - [3] C. K. Sinclair et al., Dramatic Reduction of DC Field Emission From Large Area Electrodes By Plasma-Source Ion Implantation, Thomas Jefferson National Accelerator Facility, 2001.
 - [4] G. Fursey, Field Emission in Vacuum Microelectronics Kluwer Academic/Plenum Publishers, New York, 2005.
 - [5] M. E. Mack et al., Design Issues in Gas Cluster Ion Beamlines, Epion Corporation, 2002.